22

Phospholipids at Liquid–Liquid Interfaces and Their Effect on Charge Transfer

LASSE MURTOMÄKI Department of Chemical Technology, Helsinki University of Technology, Espoo, Finland

JOSÉ A. MANZANARES and SALVADOR MAFÉ Department of Thermodynamics, University of Valencia, Burjasot, Valencia, Spain

KYÖSTI KONTTURI Department of Chemical Technology, Helsinki University of Technology, Espoo, Finland

I. INTRODUCTION

Phospholipid monolayers provide a convenient model system for studying molecular interactions in the lipid backbone of biomembranes [1,2]. Traditionally, monolayers are studied by Langmuir techniques, i.e., spreading them on an aqueous surface and following the surface pressure of the film as a function of the monolayer compression. The advantage of spreading a monolayer on an water–oil interface is that due to weaker cohesion among the hydrocarbon chains of lipid molecules, interactions can be followed over a larger range of molecular separations [3]. Langmuir film studies of phospholipids have given valuable information of the phase transitions of the lipids as a function of monolayer composition, temperature, and the aqueous phase composition and pH [4].

In the study of ion transfer across a lipid monolayer, electrochemical methodology becomes more convenient than Langmuir techniques. This is accomplished by the use of an organic solvent phase which allows sufficient dissociation of organic salts into free ions and is nonpolar enough to prevent significant partitioning of aqueous electrolytes. Monolayers are then either adsorbed on the interface from the bulk organic phase or directly added to the interface after which the establishing of an adsorption equilibrium has to be waited for, which may take several hours. Electrochemical studies of phospholipids deposited at the interface between two immiscible electrolyte solutions (ITIES) have recently been reviewed by Kakiuchi [5] who has also mostly been responsible for the work carried out in this area during the last two decades.

This chapter is basically divided in two parts, namely, the study of surface pressure–molecular area ($\pi - A$) isotherms of phospholipids at ITIES and their effect on ion transfer. In the first part, the emphasis is put on topics which have been left out from Ref. [5], i.e., Langmuir film techniques and theoretical modeling of $\pi - A$ isotherms, as well as on the latest progress in the field, especially on experiments that combine Langmuir techni-

ques with electrochemical methods. In the second part, the emphasis is put on the theoretical background of the description of interfacial ion transfer and how the perturbation of the electrical double layer at the ITIES due to the adsorbed phospholipids can modify the rate of ion transfer.

The effect of the phospholipids on the rate of ion transfer has been controversial over the last years. While the early studies found a retardation effect [6–8], more recent ones reported that the rate of ion transfer is either not retarded [9,10] or even enhanced due to the presence of the monolayer [11–14]. Furthermore, the theoretical efforts to explain this effect were unsatisfactory. The retardation observed in the early studies was explained in terms of the blocking of the interfacial area by the phospholipids, and therefore was related to the size of the transferring ion and the state of the monolayer [8,15]. The enhancement observed in the following years was attributed to electrical double layer effects, but a Frumkin-type correction to the Butler–Volmer (BV) equation was found unsuitable to explain the observations [11,16]. Recently, Manzanares et al. showed that the enhancement can be described by an electrical double layer correction provided that an accurate picture of the electrical double layer structure is used [17]. This theoretical approach will be the subject of Section III.C.

II. π–A ISOTHERMS AT LIQUID–LIQUID INTERFACES

A. Literature Review

The first modern studies of phospholipids at the water–oil interface date to the 1960s when Brooks and Pethica constructed a Langmuir trough which was operated at the water–oil interface [18]. Later, a systematic study of isotherms of the lecithin (phosphatidylcholine) monolayers at the aqueous NaCl–*n*-heptane interface was carried out in two collaborative research groups at Unilever research laboratories and in Washington University, St. Louis (see, e.g., Refs 3,19, and 20, and references therein). Based on over 2000 isotherm runs, the phase transition from the liquid expanded to the liquid condensed state (Fig. 1) was concluded to be of second order in character [3] (see Section II.C). At surface pressures below the transition point, π–A isotherms were reported to be independent of the length of the acyl chain and salt concentration or pH of the aqueous phase, but dependent on the temperature and the polar headgroup [19]; in the last case a comparison was made with cephalin with the same acyl chain length [3]. This high area behavior could not be completely explained, but was partly accounted for by dipole–dipole interactions of the zwitterionic headgroup [19,20]. The transition point was shifted towards lower surface pressures and higher molecular areas as the chain length was increased (see Fig. 2). The heat (enthalpy) of phase transition, as calculated from the 2D Clapeyron equation

$$\Delta H = T(A_t - A_S)d\pi/dT \tag{1}$$

also increased with the increasing chain length from ca. 20 to 100 kJ mol^{-1} [20]. In Eq. (1), A_t is the molecular area of the lipid at the transition, A_S is the molecular area in the solid lipid phase, taken as 47 $Å^2$, and T is the absolute temperature.

The next development on water–oil isotherms was presented by Möhwald's group at the Max-Planck Institute in Berlin [21,22]. They investigated monolayers of dipalmitoyl phosphatidylethanolamine (DPPE) at interfaces of water and hydrocarbons *n*-dodecane (C_{12}, *n*-hexadecane (C_{16}), and bicyclohexyl (BCH). The transition pressure was increased and the molecular area at transition decreased in the order C_{16}–C_{12} – BCH. Also the heat of transition was decreased in the same order, and was more strongly decreasing with

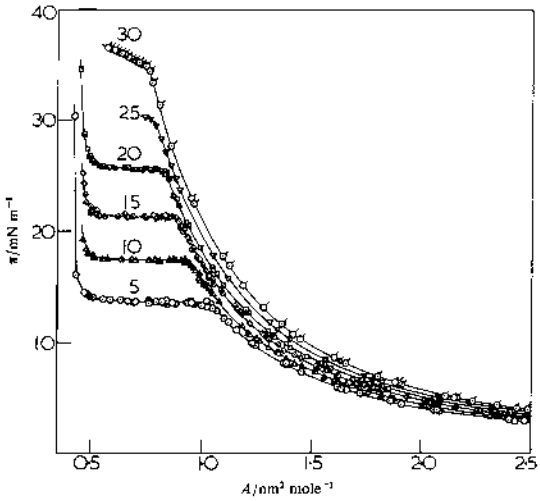

FIG. 1 π–A isotherms for 1,2-distearoyl lecithin at the water–*n*-heptane interface at different temperatures (°C, shown on the curves). (Reproduced from Ref. 20 with permission from The Royal Society of Chemistry.)

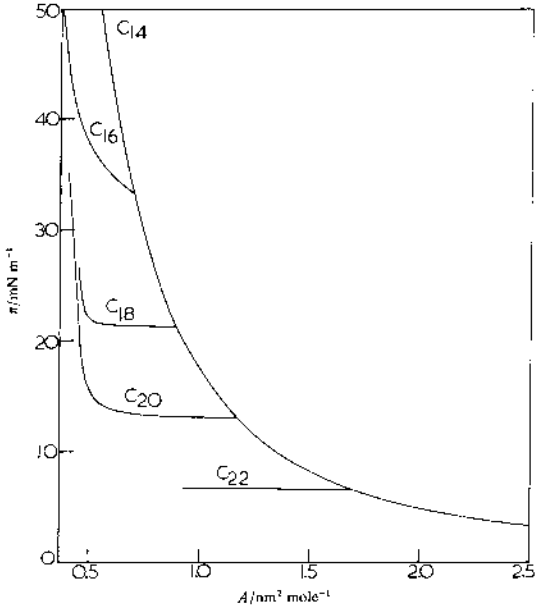

FIG. 2 Composite plot of π–A isotherms for various-chain-length lecithins typically at 20°C (Reproduced from Ref. 20 with permission from The Royal Society of Chemistry.)

temperature as in the case of *n*-heptane [20]. These phenomena were interpreted by a stabilization of the ordered phase [21] so that longer-chain alkanes created a more stable ordered phase.

During the isotherm runs, fluorescence micrographs were taken [21,22]. The micrographs clearly showed that in the plateau region of the lipid, aggregates were formed whose size increased as the compression proceeded. In the case of C_{16}, the aggregates were not of a regular shape and fused together rather easily, while in the other cases the aggregates were round and repelled each other. It was concluded that C_{16} was dissolved in the condensed phospholipid phase and squeezed out on further compression. For C_{12} and BCH a pure lipid phase was readily achieved on compression. This was explained by the size of the solvent molecules: hydrocarbons with the same length as the aliphatic tail of the lipid accommodate themselves between the tails also in an ordered phase.

Since optical measurements of monolayers at the water–oil interface are rather difficult to carry out, a configuration was suggested where a monolayer at the water–air interface was in contact with an oil lens which was partly wetting the monolayer [23]. The thermodynamic relation between this monolayer and that residing at the water–oil interface was discussed. This configuration was utilized in the X-ray diffraction experiments [24] where the structural changes of dipalmitoyl phosphatidylcholine (DPPC) and DPPE were followed.

The interfacial tension of the water–oil interface can easily and accurately be measured by the axisymmetrical drop shape analysis of the image of a pendant drop [25] whose size can be controlled. Li et al. [26] introduced this technique in the study of DPPC monolayer at the water– *n*-dodecane interface. The advantage of the pendant drop techniques is that dynamics of the lipid organization can more easily be followed than in a Langmuir trough. The isotherm obtained agreed with that measured in a Langmuir trough. Recently, Wege et al. [27] described a complete apparatus similar to that of Ref. [26], and showed isotherms of distearoyl phosphatidylcholine (DPSC) and DPPC. No proper dynamic experiments were, however, performed. Quite recently, Allen et al. [28] followed the relaxation of the DSPC monolayer at the water–1,2-dichloroethane (DCE) interface as a function of the interfacial Galvani potential difference and lipid concentration. These experiments are described in greater detail in the next section.

B. Novel Experimental Techniques

The area of the lipid covered interface can be adjusted in a very precise fashion as mentioned above [28]. In the method [9], a microsized aqueous droplet is formed at the tip of a microsyringe by extrusion into an organic phase, 1,2-DCE. The size of the droplet can be stepped via a syringe plunger connected to a piezoelectric driver. Electrodes are placed in the two solvent phases containing some appropriate electrolyte. On expansion of the droplet, a current transient is observed where the first 50 ms can be assigned to the charging of the freshly formed interface after which current decays under diffusion control. The direction of the current depends on the cell potential, and the potential where the sign of the current changes can be regarded as the potential of zero charge. On contraction a current transient with the opposite sign is observed.

After addition of lipid DSPC into the organic phase a monolayer is formed at the interface, and the steady-state current increased at all potentials. On expansion, the time constant of the charging current is reduced to ca. 5 ms and a shift of ca. 100 mV is observed in the potential of zero charge. From the video image of the droplet a highly distorted and heterogeneous interface is seen which relaxes after the fast stage (a few

seconds) very slowly. A smooth interface is observed again after ca. 20 min. For the quantitative determination of the relaxation dynamics a method was developed where an air bubble is dispersed inside the microsyringe. Hence the changes of the interfacial tension are reflected in the vapor pressure (or size) of the air bubble [29].

Dynamic surface tension has also been measured by quasielastic light scattering (QELS) from interfacial capillary waves [30]. It was shown that QELS gives the same result for the surface tension as the traditional Wilhelmy plate method down to the molecular area of 70 $Å^2$. QELS has recently utilized in the study of adsorption dynamics of phospholipids on water–1,2-DCE, water–nitrobenzene and water–tetrachloromethane interfaces [31]. This technique is still in its infancy in liquid–liquid systems and its true power is to be shown in the near future.

C. Theoretical Modeling

There is an abundance of literature on theoretical – usually statistical mechanical – models to describe phase transitions of amphiphilic monolayers; these phenomena have been reviewed by Bell et al. [32]. Bell and coworkers [33] were first to interpret the second-order phase transitions of lecithins observed at the water–oil interface [3,19] with a lattice gas model. By the second-order transition is meant a discontinuity in the slope $d\pi/dA$ without an associated discontinuity in the monolayer density. In their model, lipid molecules could have two different orientations. Molecules with similar orientation had attractive, and in the opposite orientation, repulsive interaction energy. In the model, there was also an orientation-independent energy term which might take positive or negative values [33]. Interactions only with the nearest neighbors were considered. The co-ordination number z, i.e., the number of nearest neighbors, was taken to be six, corresponding to a 2D triangular lattice. The model was able to explain the observed phase transitions only qualitatively due to simplifications and the statistical approximations made. The difference between the "expanded" and "condensed" state was shown to be the degree of order, defined as $(N_2/N_1)^{1/z}$, where N_1 and N_2 are the numbers of molecules in different orientations. The interaction energy parameters mentioned above were temperature dependent, indicating that they should be regarded as free energies with an entropy term included, rather than as simple energy parameters.

The lattice gas model of Bell et al. [33] neither gave any detailed mechanism of the orientational ordering nor separated the contributions of the headgroup and the acyl chain. Lavis et al. [34] discussed Ref. 33 critically and concluded that the sharp kink point in the isotherm at transition was an artifact of the mean field approximation used. An improved correspondence to experimental data was claimed by the use of the real-space renormalization group method [35]. The same authors returned to the problem [35] and concluded that in addition to the orientation of the molecules, chain melting had to be included in a model which could interpret the phase transitions.

In monolayers of charged or zwitterionic amphiphiles, electrostatic interactions become important because they extend over longer range than the nearest neighbors. Stigter and Dill [36,37] considered the low surface pressure region of the isotherms of Ref. 19. Based on the temperature dependence of the coefficients which were determined fitting the experimental data to a virial equation of state, the orientation of the electrical dipole moment of phosphatidylcholine (PC) or phosphatidylethanolamine (PE) headgroups at the water–*n*-heptane interface was studied. It was concluded that the ammonium group at the end of the headgroup becomes increasingly submerged in the oil phase with increasing temperature which gives raise to a strong repulsive force between the PC head-

groups. For the PE headgroup orientation is weaker which results in smaller lateral repulsion, explaining also the higher melting temperature of high-density PE monolayers.

Cantor and Dill [38] worked out a theoretical model for the interaction among the phospholipids in bilayers and monolayers that considers four area-dependent contributions to the interfacial free energy: the two-dimensional (2D) translation of the surfactants in the plane of the interface due to the 2D entropy of mixing of the surfactants with solvent, the headgroup interactions, the intramolecular interactions due to the chain configurations, and the volume dependence of chain packing. The theoretical approach can describe quantitatively the pressure–area isotherms and phase transitions of monolayers of lecithins having different chain lengths as well as predict temperatures, area, volume changes, and enthalpies of melting of the corresponding bilayers.

Ruckenstein and Li proposed a relatively simple surface pressure–area equation of state for phospholipid monolayers at a water–oil interface [39]. The equation accounted for the clustering of the surfactant molecules, and led to second-order phase transitions. The monolayer was described as a 2D regular solution with three components: singly dispersed phospholipid molecules, clusters of these molecules, and sites occupied by water and oil molecules. The effect of clusterng on the theoretical surface pressure–area isotherm was found to be crucial for the prediction of phase transitions. The model calculations fitted surprisingly well to the data of Taylor et al. [19] in the whole range of surface areas and the temperatures (Fig. 3). The number of molecules in a cluster was taken to be 150 due to an excellent agreement with an isotherm of DSPC when this

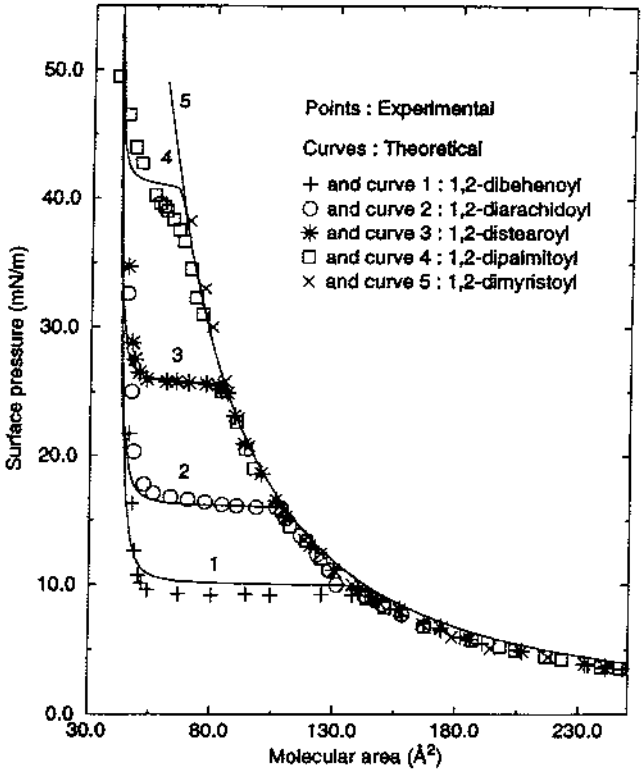

FIG. 3 π–A isotherms measured for five lecithins at 15°C. (Experimental data from Ref. 20. Reproduced from Ref. 39 with permission from The American Chemical Society.)

number was used. The free energy of transfer of a lipid molecule from singly dispersed state to the bulk of a cluster varied between -4 kJ mol^{-1} (C_{14}) and -25 kJ mol^{-1} (C_{22}), decreasing slightly with increasing temperature.

Mafé et al. considered the phospholipid adsorption and surface pressure–area isotherms at interfaces using two models that incorporated a minimum number of adjustable parameters and predicted first-order phase transitions [40]. The first model was based on the 2D lattice statistics of binary solutions and the molecular parameters introduced were the energy change involved in the mixing process of the phospholipid and organic solvent molecules and the phospholipid head effective area. The state of aggregation of the lipids at the interface was showed by evaluating the difference in the number of solvent–lipid interactions between a random distribution of lipids and that predicted by a quasichemical approximation. The second model made use of a nonlocalized adsorption model for the calculation of the surface concentration of the phospholipids at the interface as a function of the volume concentration in the organic solvent phase, and a 2D hard disks gas model with a mean-field term accounting for the attractive interactions between the tails of the adsorbed phospholipids. The equation of state predicted by this second model was the 2D van der Waals (vdW) equation

$$\left(\pi + \frac{u_0 A_{ex}}{2A^2}\right)(A - A_{ex}) = kT \tag{2}$$

where A_{ex} is the excluded area of a phospholipid head and u_0 is the interaction energy between the phospholipid tails. When the theoretical results were compared with experimental data for the water–1,2-DCE and water–air interfaces [41], the two models appeared to predict correctly the qualitative features of the experimental isotherms (Fig. 4).

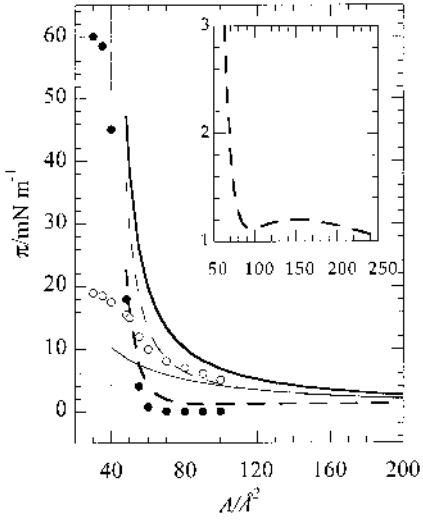

FIG. 4 π–A isotherms measured for DSPC at water–1,2-DCE (○) and water–air (●) interfaces from Ref. 41 and simulated with a real gas model [40]: ideal gas with $A_{ex} = 0$ and $u_0 = 0$ (thin solid line), hard disks gas with $A_{ex} = 40$ Å^2 and $u_0 = 0$ (thick solid line), vdW gas with $A_{ex} = 40$ Å^2 and $u_0/kT = 3$ (thin dashed line), and vdW gas with $A_{ex} = 40$ Å^2 and $u_0/kT = 7$ (thick dashed line). The inset shows part of the thick dashed line. (Reproduced from Ref. 40 with permission from Elsevier Science.)

III. ION TRANSFER ACROSS ITIES IN THE PRESENCE OF ADSORBED PHOSPHOLIPIDS

A. Literature Review

Monolayers of organic surfactants at water–air interfaces are known to decrease the rate of solute transfer across them [42,43]. Similarly, the studies on ion transfer across lecithin and protein monolayers at ITIES found a retardation effect [6–8]. The first studies of ion transfer across monolayers of pure lipids at ITIES showed that the state of monolayer has a great effect on the rate of ion transfer. Monolayers in an expanded state appeared to be completely transparent to the transfer of small ions [5], while those in a condensed state decreased the rate of ion transfer. Long hydrophobic tails (large attractive interaction between lipids), low temperatures, and large size of the transferring ion were identified as factors decreasing the rate of ion transfer [11,15]. Hence, the blocking effect observed with egg yolk lecithin monolayers could be attributed to the fact that this mixture of natural phospholipids forms a more closely packed structure than pure lipids.

In some cases, an acceleration of the rate of ion transfer was observed [12]. Kakiuchi et al. [11,16] studied by AC impedance perchlorate, tetramethylammoniun (TMA^+), and tetraethylammonium (TEA^+) ion transfer across water–nitrobenzene interfaces covered by different PCs in the temperature range $5°C < t < 30°C$. Short-tail lipids, such as DLPC and DPPC, showed a clear enhancement of the rate of ion transfer (Fig. 5).

Kontturi et al. studied TEA^+ ion transfer across water–1,2-DCE microinterfaces covered by different PCs using short potential step techniques [12]. The enhancement in the forward rate constant was observed for all lipids and increased with the surface coverage (Fig. 6).

Chesniuk et al. studied the transfer of alkali and alkaline-earth cations across phospholipid monolayers at water–1,2-DCE macrointerfaces by cyclic voltammetry. These authors considered the effect of the cation nature, the concentration of the transferring ion, and the applied potential (at the positive end of the polarization window), and noticed either an enhancement of the current or a blocking of the transfer process [13,14]. The enhancement factors observed were very much larger than in other studies, especially at

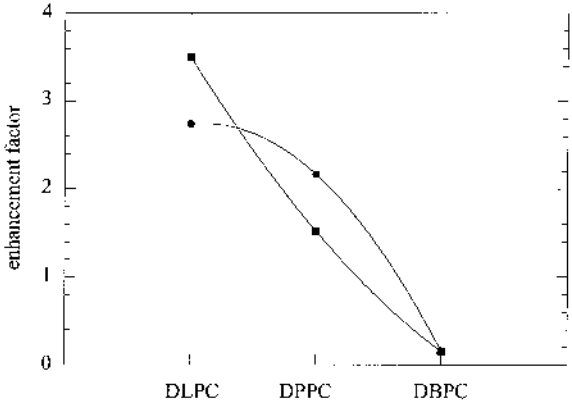

FIG. 5 Enhancement factor observed in the forward rate constant for TMA^+ (●) and TEA^+ (■) ion transfer at the water-nitrobenzene interface due to the presence of different PCs. (Experimental data are taken from Ref. 11 and correspond to 30°C.)

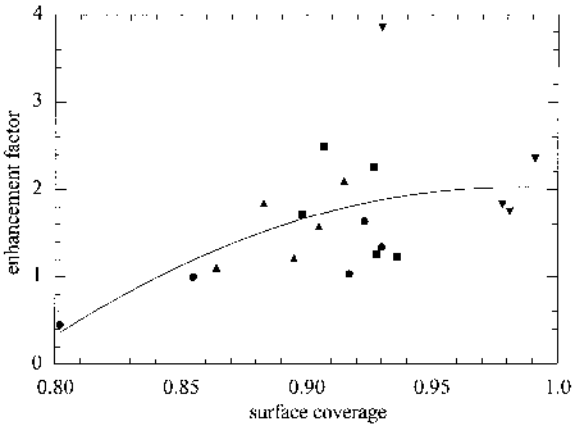

FIG. 6 Enhancement factor observed in the forward rate constant for TEA^+ ion transfer at the water–1,2-DCE interface due to the presence of PCs: DLPC (●), DMPC (■), DPPC (▲), and DSPC (▼). (Experimental data are taken from Ref. 12.)

low applied potentials and at low concentrations of the transferring ion. A noteworthy difference between this and previous studies is that the transfer of the supporting electrolyte ions themselves, and not a tracer ion added to the supporting electrolyte solution, was studied.

B. Novel Experimental Techniques

Since the state of the lipid layer was known to have a great effect on the rate of charge transfer through the layer, Grandell and Murtomäki designed a novel type of Langmuir trough to achieve simultaneous electrochemical and surface pressure control [41]. Organic solvent phases previously used in the liquid–liquid Langmuir troughs are electrochemically unsuitable because they either do not dissolve electrolytes or exhibit a narrow polarization window. 1,2-DCE was used as the organic phase and isotherms of the DSPC monolayer were measured. Due to the high solubility of the lipid in the organic phase, or the high mobility of the small solvent molecules within the film, the surface pressure remained rather low, ca. 20 mN m^{-1}, at maximum compression. In the subsequent paper [10] isotherms were recorded under potential control and the observed potential dependent adsorption of the lipid agreed with that measured earlier [44]. The effect of the monolayer on the transfer rate of the two probe ions, cationic propranolol and anionic picrate, was practically insignificant, even at maximum values of surface pressure reached [45].

An inherent problem with the electrochemical Langmuir trough is its uneven potential distribution [45]. Therefore, a Langmuir–Blodgett approach was designed to achieve a known surface pressure for the film under study. A lipid film is spread at the water–air interface and compressed to a desired surface pressure, after which an electrochemical cell containing an *o*-nitrophenyltoctylether gel is dipped through the film into the aqueous phase. A lipid film is transferred on the top of the gel thus forming a lipid coated liquid–liquid interface [46]. Preliminary results show the retardation of the propranolol transfer, whereas the rate of TEA^+ cation remained unaltered.

More recently, Manzanares et al. [17] presented additional experimental evidence of the enhanced cation transfer across a hemispherical water–1,2-DCE interface covered with DSPC by using a syringe experimental set up described elsewhere [9,28]. Figure 7 shows the cyclic voltammograms measured in the cell [17],

Ag	AgTPBCl$_4$	20 mM TPeATPBCl$_4$		1 M LiCl, 1 mM CO_3^{2-}/HCO_3^-	AgCl	Ag
(s)	(s)	(1,2-DCE)		(aq.)	(s)	(s)

before (a) and after (b) the addition of DSPC. The organic supporting electrolyte is tetrapentylammonium tetrakis-(4-chlorophenyl)borate. The carbonate–bicarbonate buffer sets the pH at 8.7, where the headgroup of this phospholipid is in zwitteronic form. It is observed that the current density increases at both sides of the window. At the positive side of the window, Li^+ ion transfer from the aqueous to the organic phase. The enhancement factor (i.e., the ratio of current densities) observed for Li^+ ion tranfer varies slightly with cell potential, and takes values between 5 and 10, thus being of the same order as those observed in Refs. 11 and 12.

An analogous apparatus to that of Ref. 9 was used to follow the effect of the lipid monolayer on the rate of electron transfer (ET). In this setup [47], an organic phase droplet (1,2-DCE) is continuously expanded into the aqueous phase, and the resulting current transient was monitored in the absence and presence of the adsorbed lipid monolayer. The rate of ET was decreased as a function of the lipid concentration.

Perhaps the most important experimental progress made recently in electrochemistry was the introduction of a scanning electrochemical microscope (SECM). Tsionsky et al. have used SECM to study also the rate of ET across a lipid monolayer at the water–benzene interface [48,49]. The presence of the monolayer decreased the rate of ET, being the decrease more significant for longer hydrocarbon chains and larger lipid concentration in solution. It was thus concluded that the ET reaction does not occur at defect sites in the lipid monolayer.

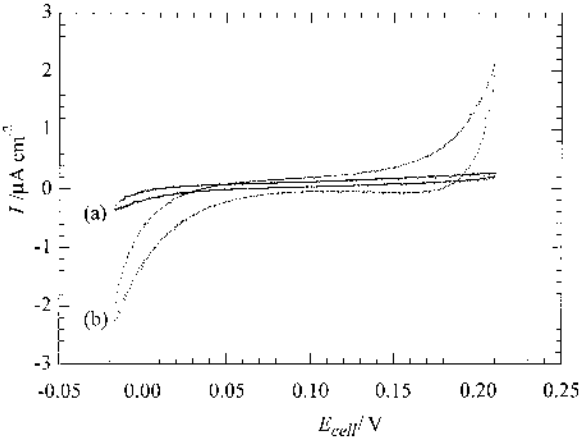

FIG. 7 Comparison of cyclic voltammograms recorded at 1 mV/s before (a) and after addition (b) of 59 μM DSPC to the organic phase. (Reproduced from Ref. 17 with permission from Elsevier Science.)

C. Theoretical Modeling

1. Kinetics of Interfacial Ion Transfer

The description of the ion transfer process is closely related to the structure of the electrical double layer at the ITIES [50]. The most widely used approach is the combination of the BV equation and the modified Verwey–Niessen (MVN) model. In the MVN model, the electrical double layer at the ITIES is composed of two diffuse layers and one ion-free or inner layer (Fig. 8). The positions delimiting the inner layer are denoted by x_2^o and x_2^w, and represent the positions of closest approach of the transferring ion to the ITIES from the organic and aqueous side, respectively. The total Galvani potential drop across the interfacial region, $\Delta_o^w\phi \equiv \phi^w - \phi^o$, is then decomposed as

$$\Delta_0^w\phi = \Delta\phi_d^o + \Delta_o^w\phi_2 + \Delta\phi_d^w \tag{3}$$

The elementary step of ion transfer is considered to take place between positions x_2^o and x_2^w, and therefore the electrical potential drop affecting this transfer is $\Delta_o^w\phi_2$. The ion transfer involves the renewal of the solvation shell. The change in standard chemical potential $\Delta_0^w\phi_i^0$ associated with this process takes place over very short distances in the interfacial region [51] and can be assumed to occur between positions x_2^o and x_2^w. Thus, the BV equation for the flux density J_i of an ionic species i is [52]

$$J_i = k_i^0\left[c_i(x_2^w)e^{\alpha z_i f(\Delta_o^w\phi_2 - \Delta_o^w\phi_i^0)} - c_i(x_2^o)e^{(\alpha-1)z_i f(\Delta_0^2\phi_2 - \Delta_o^w\phi_i^0)}\right] \tag{4}$$

where k_i^0 is the true standard rate constant, $c_i(x_2^w)$ and $c_i(x_2^o)$ are the molar concentrations of the transferring ion at positions x_2^w and x_2^0, z_i is its charge number, α is the forward transfer coefficient, and $f \equiv F/RT$, where F is Faraday's constant, R is the gas constant, and T is the absolute temperature.

Alternatively, the flux density J_i can be expressed in terms of the ion concentrations, c_i^w and c_i^o at the positions x_0^w and x_0^o just outside the diffuse layers, and the total Galvani potential difference $\Delta_o^w\phi$. In this case, the BV equation takes the form [53,54]

$$J_i = k_{i,\text{app}}^0\left[c_i^w e^{\alpha z_i f(\Delta_o^w\phi - \Delta_o^w\phi_i^0)} - c_i^o e^{(\alpha-1)z_i f(\Delta_o^w\phi - \Delta_o^w\phi_i^0)}\right] \tag{5}$$

where

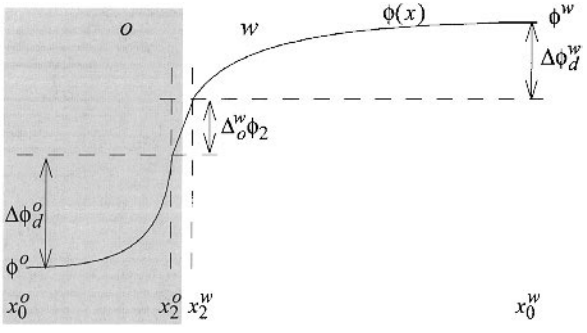

FIG. 8 Schematic representation of the electrical potential profile $\phi(x)$ at the ITIES. The potential drops are: $\Delta\phi_d^o$ in the organic diffuse layer $x_0^o < x < x_2^o$, $\Delta_o^w\phi_2$ in the inner layer $x_2^o < x < x_2^w$, and $\Delta\phi_d^w$ in the aqueous diffuse layer $x_2^w < x < x_0^w$.

$$k^0_{i,\mathrm{app}} = k^0_i e^{(1-\alpha)z_i f \Delta\phi^w_d} e^{-\alpha z_i f \Delta\phi^o_d} \tag{6}$$

is the apparent standard rate constant. Since the potential drops $\Delta\phi^w_d = \phi^w - \phi^w_2$ and $\Delta\phi^o_d = \phi^o_2 - \phi^o$ are different to each other, the apparent rate constant $k^0_{i,\mathrm{app}}$ differs from the true constant k^0_i even when $\alpha = 1/2$.

Note that Eqs. (4) and (5) implicitly consider the transfer across the interface as the rate-determining step in the ion transfer processes [51], and neglect other steps involved in the process such as the ion transport across the diffusion boundary layers [55] and across the diffuse electrical double layer [50].

2. Electrostatic Enhancement of the Ion Transfer Due to the Presence of Phospholipids

According to Eq. (5) the rate of interfacial ion transfer is determined by the rate constant k^0_i, the interfacial concentrations $c_i(x^w_2)$ and $c_i(x^o_2)$, and the potential difference $\Delta^w_0\phi_2 - \Delta^2_o\phi^0_i$. The phospholipids adsorbed at the ITIES are likely to modify one or several of the above factors, and hence the rate of ion transfer. The rate constant k^0_i depends on the nature of the transferring ion and the solvents, and would be expected to change when the phospholipid monolayer is so condensed that the state of the solvents at the interface is modified. The local concentrations $c_i(x^w_2)$ and $c_i(x^o_2)$ depend on the concentrations in the respective bulk phases and the electrical potentials ϕ^w_2 and ϕ^o_2; other effects might also become important in highly condensed monolayers. Thus, phospholipid headgroups bearing electrical charges (either net or zwitteronic charge) are expected to modify the local concentrations. Similarly, these electrical charges could also affect the value $\Delta^w_o\phi_2$.

From a practical point of view, the potential drop across the inner layer $\Delta^w_o\phi_2$ must be determined by fitting the experimental data to the equations derived from this theoretical approach, which led to some controversy about its value [53,54,56,57]. For the sake of simplicity, and also because recent studies of the ITIES structure do not confirm the presence of an inner layer [51,58], we neglect the finite size of the transferring ion and take $x^w_2 = x^o_2 = 0$ and $\Delta^w_o\phi_2 = 0$. This is equivalent to accepting that the potential difference $\Delta^w_o\phi_2 - \Delta^w_o\phi^0_i$ is not modified by the presence of the phospholipids.

Phospholipid monolayers in liquid expanded state are likely to modify mostly the interfacial concentrations, and this electrostatic effect can be described by Eq. (6). Taking $\alpha \approx 1/2$, in agreement with most experimental results, and introducing the approximation $\Delta^w_o\phi_2 = 0$, Eq. (6) simplifies to [59]

$$k^0_{i,app} = k^0_i e^{-z_i f \tilde{\phi}(0)} \tag{7}$$

where $\tilde{\phi}(0) \equiv \phi(0) - (\phi^w + \phi^o)/2$ and $\phi(0)$ is the potential at the ITIES. The exponential factor in Eq. (7) can result in either a decrease or an enhancement of the rate of ion transfer. For every value of $\Delta^w_o\phi$, we define the enhancement factor as

$$\frac{k^0_{i,app}(\mathrm{presence})}{k^0_{i\mathrm{app}}(\mathrm{absence})} = e^{-z_i f[\phi(0)_{\mathrm{presence}} - \phi(0)_{\mathrm{absence}}]} \tag{8}$$

and compare it to the ratio of currents across the ITIES in the presence and in the absence of phospholipids.

Note, finally, that condensed monolayers could also modify the true standard rate constant k^0_j, which would account for the observed partial blocking of the ion transfer [8,15]. The present study, however, is restricted to the electrostatic effect.

3. The Electrical Potential Distribution at the ITIES in the Presence of Zwitterionic Phospholipids

When a monolayer of phospholipids is adsorbed at the ITIES, there must be a modification of the electrical structure of the interface [60]. Since we aim at describing the effect of this monolayer on the rate of ion transfer in a simple way, we assume a sharp interface also in the presence of phospholipids. The hydrophobic tails are located in the organic phase (negative x region), and the hydrophilic headgroups are located in the aqueous phase (positive x region).

A key issue in the description of the monolayer is the orientation of the zwitterionic headgroups. At water–air interfaces, Standish and Pethica [61] showed that the headgroup is oriented parallel to the interface. In lipid bilayers in electrolyte solutions, however, Ashcroft et al. concluded [62] and that the phosphatidylcholine headgroup changed its orientation with respect to the membrane–solution interface from normal in 1 mM KCl to parallel in 1000 mM KCl (see also Ref. 63). Taking into account that the dipole moment of the phosphatidylcholine headgroup has been estimated to be 19 D [64], even a small inclination will produce a large effect on the electrical potential distribution at the interface. Therefore, the orientation of the headgroups might be approximately but not exactly parallel to the interface, with the negative phosphonic groups closer to the ITIES and the positive amine groups further away into the aqueous phase. Following previous work on the electrostatic properties of lipid membranes [61] and zwitteronic micelles [65,66] and surfaces [63], and considering the aqueous supporting electrolyte concentration to be in the range 10–1000 mM, we propose a value of 3 to 4 Å for the distance d between the positive and negative charges in the headgroup in the direction normal to the interface.

For the sake of simplicity, the negative phosphonic groups are considered to be located at the ITIES, $x = 0$, and therefore a negative charge density $-\sigma$ is associated to this plane. Similarly, a charge density $\sigma > 0$ is associated with the plane $x = d$ corresponding to the amine groups. Moreover, since the headgroups are likely to affect the water structure in the interfacial region, a dielectric permittivity $\varepsilon^i \approx 30\varepsilon_0$, where ε_0 is the vacuum permittivity, is considered in this region [61,67].

When the ITIES is polarized with a potential difference $\Delta_o^w\phi$, there is a separation of electrical charge across it. According to the Gouy–Chapman theory, the charges in the aqueous and organic diffuse layers are related to the potential drops $\Delta\phi_d^w$ and $\Delta\phi_d^o$ in the respective layers by the equations

$$q^w = \frac{2\varepsilon^w\kappa^w}{f}\sinh\frac{f\Delta\phi_d^w}{2} \tag{9}$$

$$q^o = -\frac{2\varepsilon^o\kappa^o}{f}\sinh\frac{f\Delta\phi_d^o}{2} \tag{10}$$

where $\kappa^w = (2F^2c^w/\varepsilon^w RT)^{1/2}$ and $\kappa^o = (2F_c^2o/\varepsilon^o RT)^{1/2}$ are the reciprocal Debye lengths in the aqueous and organic electrolyte solutions; c^w and c^o denote the concentrations of the supporting electrolytes in the respective phases. In the absence of phospholipids, the condition $q^o + q^w = 0$ allows us to evaluate the surface potential as [68,69]

$$\tilde{\phi}(0) = 2\text{arctanh}\left[\frac{r-1}{r+1}\tanh\left(\frac{f\Delta_o^w\phi}{4}\right)\right] \tag{11}$$

where $r \equiv \varepsilon^w\kappa^w/(\varepsilon^o\kappa^o)$.

The presence of the phospholipids modifies the electrical double layer and the evaluation of the surface potential $\tilde{\phi}(0)$ requires then the solution of the PB equation in the aqueous region in between the two planes of charge, $0 < x < d$ [59]. The influence of the phospholipids is expected to be the largest when the ionic strength of the solutions is low, since then there are fewer ions to screen the zwitterionic charges. Furthermore, the effect of the phospholipids is determined by the charge separation due to the polar headgroups in relation to the charge separation due to the applied potential difference $\Delta_o^w\phi$. Since the latter is larger for higher applied potentials, it is expected that the effect of the phospholipids decreases with increasing $\Delta_o^w\phi$.

Considering that the ions of the aqueous supporting electrolyte can be present in the region $0 < x < d$, the PB equation takes the form

$$f\frac{d^2\phi}{dx^2} = \kappa^{i^2}\sinh[f(\phi - \phi^w)] \tag{12}$$

where $\kappa^i = (2F^2c^w/\varepsilon^i RT)^{1/2}$ is the reciprocal Debye length of this region, and the boundary conditions for this equation are

$$\varepsilon^i\left(\frac{d\phi}{dx}\right)_{x=0+} = \sigma - q^o \tag{13}$$

$$\varepsilon^i\left(\frac{d\phi}{dx}\right)_{x=d-} = \sigma + q^w \tag{14}$$

where q^o and q^w are given by Eqs. (9) and (10) with $\Delta\phi_d^w = \phi^w - \phi(d)$ and $\Delta\phi_d^o = \phi(0) - \phi^o$.

The integration of Eq. (12) from x to $x = d-$ yields the following relation between the electrical potential $\phi(x)$ and its gradient $d\phi/dx$:

$$\left(\varepsilon^i\frac{d\phi}{dx}\right)^2 = (\sigma + q^w)^2 - r^{i^2}q^{w^2} + \left[\frac{2\varepsilon^i\kappa^i}{f}\sinh\frac{f(\phi - \phi^w)}{2}\right]^2 \tag{15}$$

where Eq. (14) has been used and $r^i \equiv \varepsilon^i\kappa^i/(\varepsilon^w\kappa^w) = (\varepsilon^i/\varepsilon^w)^{1/2}$. This equation can be used to determine the potentials $\phi(0)$ and $\phi(d)$ for given values of σ and $\Delta_o^w\phi$. The solution procedure starts with an intial guess of $\phi(0)$. Then, q^w and $\phi(d)$ can be obtained from

$$q^{w^2}(1 - r^{i^2}) - q^{o^2} + 2\sigma(q^o + q^w) = -\left(\frac{2\varepsilon^i\kappa^i}{f}\sinh\frac{f[\phi(0) - \phi^w]}{2}\right)^2 \tag{16}$$

which results from Eq. (15) applied to position $x = 0+$ and boundary condition Eq. (13). The initial guess of $\phi(0)$ is then iteratively improved until the condition

$$\int_0^d \frac{d\phi}{d\phi/dx} = d \tag{17}$$

is satisfied; note that $d\phi/dx$ can only vanish when q^w is negative and large in magnitude.

4. Simulated Enhancement Factors

The theory presented above accounts for the electrostatic effects on the apparent rate constant for ion transfer by relating the observed changes in $k^0_{i,\mathrm{app}}$ to changes in $c_i^w(0)$, or equivalently to $\phi(0)$. In the following, we present the simulated electrical potential distributions and the corresponding enhancement factors for a cation transferring from the aqueous phase across the water–1,2-DCE interface ($\varepsilon_r^w = 78.39$, $\varepsilon_r^o = 10.36$). The rela-

tive permittivity of the interfacial region is estimated as $\varepsilon_r^i = 30$, and the separation between the charged plans is $d = 3$Å. The surface charge concentration σ is expressed as a molecular area for the zwitterionic headgroups, with values ranging from condensed ($a = 50$ Å^2, $\sigma = 32.0$ μC/cm^2) to very dilute ($a = 150$ Å^2, $\sigma = 10.7$ μC/cm^2) monolayers.

Figure 9 shows the electrical potential and the space charge density profiles for concentrations $c^w = 1000$ mM and $c^o = 20$ mM and Galvani potential difference $f\Delta_o^w\phi = 5$ in the absence (a) and in the presence (b) of a phospholipid monolayer with a molecular area of 150 Å^2 ($\sigma = 10.7$ μC/cm^2). The ITIES has been marked with a continuous vertical line, and the plane where amine groups are assumed to be located has been marked with a dashed line. The potential distributions in the region $0 < x < d$ are nonlinear due to the presence of aqueous ions. The phosphonic groups located at the ITIES makes the potential $\phi(0)$ smaller in case (b) than in case (a), which according to Eq. (8) implies an enhancement of the rate of ion transfer. The space charge density profiles shown in Fig. 9 evidence clearly how strongly the presence of the phospholipids modifies the ionic concentrations close to the ITIES. In particular it is observed that the charge density in the aqueous phase is positive in the absence of phospholipids (note that $\Delta_o^w\phi > 0$) and becomes then large and positive in the interfacial region $0 < x < d$ and negative in the aqueous phase $x > d$ when the phospholipids are present. From the integration of these profiles the charge distribution in the different regions can be evaluated as $q^o = -q^w = -2.85$ μC/cm^2 in case (a) and $q^o = -1.06$ μC/cm^2, $q^w = -4.40$ μC/cm^2, $q^i = 5.46$ μC/cm^2 in case (b), which indicates that the excess positive charge in the interfacial region is of the same order as the charge density σ associated with the headgroups. Hence, the enhancement of the rate of ion transfer is attributed to a significant increase of the interfacial concentration of the transferring ion.

Figure 10 shows the enhancement factor, $e^{-z_i f[\phi(0)_{\text{presence}} - \phi(0)_{\text{absence}}]}$, theoretically predicted for the concentrations $c^w = 1000$ mM, $c^o = 20$ mM and different values of the phospholipid molecular area. The potential different varies from $\Delta_o^w\phi = 0$ to $10/f \approx$

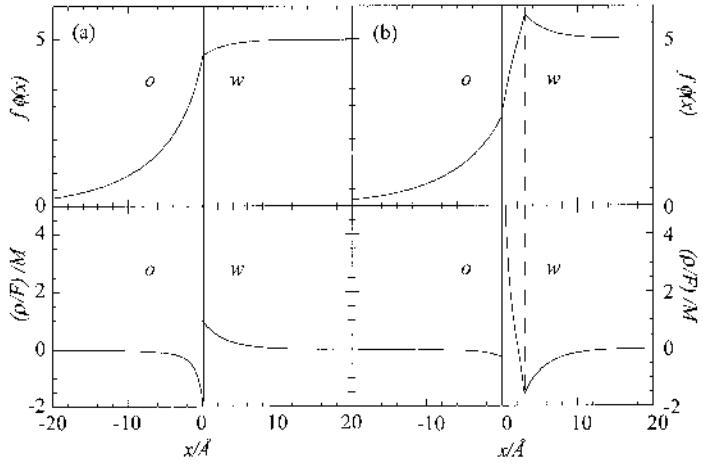

FIG. 9 Simulated electrical potential and space charge density profiles at the water–1,2-DCE interface polarized at $f\Delta_o^w\phi = 5$ in the absence (a) and in the presence (b) of zwitterionic phospholipids. The supporting electrolyte concentrations are $c^o = 20$ mM and $c^w = 1000$ mM. The molecular area of the phospholipids is 150 Å^2, and the corresponding surface charge density is $\sigma = 10.7$ μC/cm^2. The distance between the planes of charge associated with the headgroups is $d = 3$ Å.

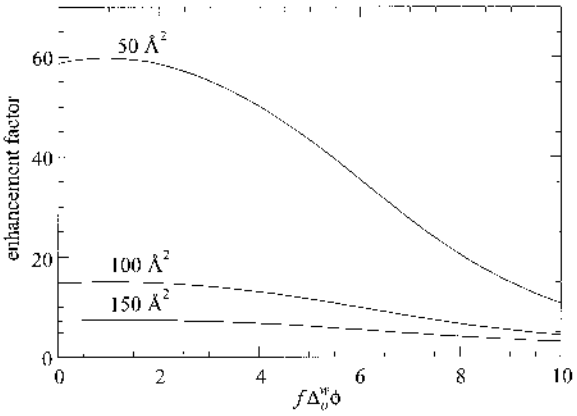

FIG. 10 Simulated enhancement factor for monolayers of zwitterionic phospholipids with different molecular areas (shown on the curves) at the polarized water–1,2-DCE interface. The supporting electrolyte concentrations are $c^o = 20$ mM and $c^w = 1000$ mM.

257 mV at 25°C. As could be expected, the enhancement factor is larger when the surface charge density σ associated to the phospholipids is large compared to the charge density $q^o = -q^w$ separated across the ITIES due to $\Delta_o^w\phi$ (in the absence of phospholipids). These results are in agreement with the experimental observations in Refs. 11 and 13.

Figure 11 analyzes the effect of the electrolyte concentration in the aqueous phase, for fixed electrolyte concentrations in the organic phase $c^o = 10$ mM and 50 mM, and a Galvani potential difference $f\Delta_o^w\phi = 5$. These theoretical results are in agreement with the observations in Ref. 13. Moreover, it is shown that a decrease in the electrolyte concentration in the organic phase has a similar effect to a decrease in the electrolyte concentration in the aqueous phase.

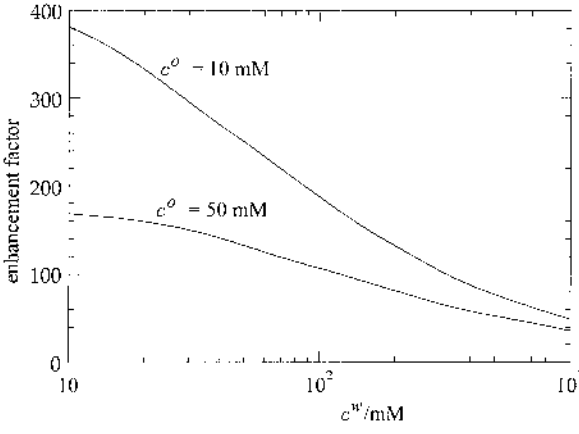

FIG. 11 Simulated enhancement factor against electrolyte concentration in aqueous phase. The potential different across the water–1,2-DCE interface is $f\Delta_o^w\phi = 5$ and the electrolyte concentration in the organic phase is $c^o = 10$ mM and 50 mM. The phospholipid molecular area is 50 Å^2.

IV. CONCLUSIONS

Phospholipid monolayers at liquid–liquid interfaces influence the charge transfer processes in two ways. On the one hand, the phospholipids constitute a barrier that blocks the process by impeding the transferring species to reach the interface [1,15,48]. On the other hand, the phospholipids modify the electrical potential difference governing the process [60]. While the first influence invariably leads to a decreased rate, the second one might result in either a decreased or an increased rate of charge transfer. The net effect of the phospholipids on the charge transfer process depends on the state of the monolayer, and therefore studies with simultaneous electrochemical and surface pressure control are preferable [10,41,45].

The effect of phospholipid monolayers on the rate of charge transfer has been the subject of several experimental studies, but still there is a need for additional experimental evidence. For large molecular areas, the effect on the rate of ion transfer seems to be negligible [5]. An increasing surface concentration of lipids leads to liquid expanded states where the electrostatic effects are noticeable. An enhanced rate of ion transfer across monolayers of pure phospholipids has then been observed both for the cases of tracer [11,12] and supporting electrolyte ion transfer [13,17]. Finally, the blocking effect is dominant in liquid condensed monolayers [15].

A theoretical approach based on the electrical double layer correction has been proposed to explain the observed enhancement of the rate of ion transfer across zwitterionic phospholipid monolayers at ITIES [17]. If the orientation of the headgroups is such that the phosphonic group remains closer to the ITIES than the ammonium groups, the local concentration of cations is increased at the ITIES and hence the current observed due to cation transfer is larger than in the absence of phospholipids at the interface. This enhancement is evaluated from the solution of the PB equation, and calculations have been carried out for the conditions of the experiments presented in the literature. The theoretical results turn out to be in good agreement with those experimental studies, thus showing the importance of the electrostatic correction on the rate of ion transfer across an ITIES with adsorbed phospholipids.

This type of theoretical analysis has been used also to study the effect of ionic surfactants and coadsorbed layers on the rate of ion transfer and the theoretical results have been again in agreement with experimental observations [59]. Thus, other experimental situations might be analyzed similarly. However, some comments must be stressed. The electrical double layer correction is based on the Gouy–Chapman theory, which leads to unrealistically high interfacial concentrations in most cases and therefore might overrestimate the enhancement factor. More importantly, other effects such as steric hindrance, giving rise to partial blocking of ion transfer are expected to overcome the electrostatic effects in condensed monolayers.

ACKNOWLEDGMENTS

Financial support from the European Union under project No. FMRX-CT96-0078 and from the Ministry of Education and Culture of Spain under DGICYT project No. PB98-0419 is acknowledged. L. M. acknowledges the Academy of Finland for the research position.

REFERENCES

1. M. Blank and J. S. Britten, in *Physical Principles of Biological Membranes* (F. Snell, J. Wolken, G. Iverson and J. Lam, eds.) Gordon and Breach, New York, 1970, pp. 143–163.
2. M. Blank, in *Progress in Surface and Membrane Science*, vol. 13 (D. A. Cadenhead and J. F. Danielli, eds.) Academic Press, New York, 1979, pp. 87–139.
3. B. Y. Yue, C. M. Jackson, J. A. G. Taylor, J. Mingins, and B. A. Pethica. J. Chem. Soc. Faraday Trans. 1 *72*:2685 (1976).
4. P. M. Phillips and D. Chapman. Biochim. Biophys. Acta *163*:301 (1968).
5. T. Kakiuchi, in *Liquid–Liquid Interfaces. Theory and Methods* (A. G. Volkov and D. W. Deamer, eds.) CRC Press, Boca Raton, 1996, pp. 317–331.
6. J. Koryta, L. Q. Hung, and A. Hofmanova. Stud. Biophys. *90*:25 (1982).
7. H. H. J. Girault and D. J. Schiffrin, in *Charge and Field Effects in Biosystems* (M. J. Allen and P. N. R. Usherwood, eds.), Abacus Press, Tunbridge Wells, 1984, pp. 171–178.
8. V. J. Cunnane, D. J. Schiffrin, M. Fleischmann, G. Geblewicz, and D. Williams. J. Electroanal. Chem. *243*:455 (1988).
9. R. M. Allen and D. E. Williams. Faraday Discuss. *104*:281 (1996).
10. D. Grandell, L. Murtomäki, K. Kontturi, and G. Sundholm, J. Electroanal. Chem. *463*:242 (1999).
11. T. Kakiuchi, M. Kotani, J. Noguchi, M. Nakanishi, M. Senda. J. Colloid Interface Sci. *149*:279 (1992).
12. A. K. Kontturi, K. Kontturi, L. Murtomäki, B. Quin, and V. J. Cunnane. J. Electroanal. Chem. *424*:69 (1997).
13. S. G. Chesniuk, S. A. Dassie, L. M. Yudi, and A. M. Baruzzi. Electrochim. Acta *43*:2175 (1998).
14. S. G. Chesniuk, S. A. Dassie, L. M. Yudi, and A. M. Baruzzi. Langmuir *14*:5226 (1998).
15. T. Kakiuchi, T. Kondo, and M. Senda. Bull. Chem. Soc. Jpn. *63*:3270 (1990).
16. T. Kakiuchi, T. Kondo, M. Kotani, and M. Senda. Langmuir *8*:169 (1992).
17. J. A. Manzanares, R. M. Allen, and K. Kontturi. J. Electroanal. Chem., *483*:188 (2000).
18. J. H. Brooks and B. A. Pethica. Trans Faraday Soc *60*:208 (1964).
19. J. A. G. Taylor, J. Mingins, and B. A. Pethica. J. Chem. Soc. Faraday Trans. 1 *72*:2694 (1976).
20. J. Mingins, J. A. G. Taylor, B. A. Pethica, C. M. Jackson, and B. Y. Yue. J. Chem. Soc. Faraday Trans. 1 *78*:323 (1982).
21. M. Thoma and H. Möhwald. J. Colloid Interface Sci. *162*:340 (1994).
22. M. Thoma and H. Möhwald. Colloids Surf. A *95*:193 (1995).
23. M. Thoma, T. Pfohl, and H. Möhwald. Langmuir *11*:2881 (1995).
24. G. Brezinski, M. Thoma, B. Struth, and H. Möhwald. J. Phys. Chem. *100*:3126 (1996).
25. S. Hartland and R. W. Hartley, *Axisymmetric Fluid–Liquid Interfaces*, Elsevier, Amsterdam, 1976.
26. J. Li, R. Miller, R. Wüstneck, H. Möhwald, and A. W. Neumann. Colloids Surf. A *96*:295 (1995).
27. H. A. Wege, J. A. Holgado-Terriza, M. J. Gálvez-Ruiz, and M. A. Cabrerizo-Vilchez. Colloids Surf. B *12*:339 (1999).
28. R. M. Allen, K. Kontturi, L. Murtomäki, and D. E. Williams. J. Electroanal. Chem. *483*:57 (2000).
29. R. M. Allen, D. E. Williams, and K. Kontturi, Electrochem. Comm. accepted.
30. B. S. Sauer, Y.-L. Chen, G. Zografi, and H. Yu. Langmuir *2*:683 (1986).
31. Z. Zhang and T. Sawada, in *Euroconference on Modern Trends in Electrochemistry of Molecular Interfaces*, Kirkkonummi, Finland, 1999, P-45.
32. G. M. Bell, L. L. Combs, and L. J. Dunne. Chem. Rev. *81*:15 (1981).
33. G. M. Bell, J. Mingins, and J. A. G. Taylor. J. Chem. Soc. Faraday Trans. 2 *74*:223 (1978).
34. D. A. Lavis, B. W. Southern, and G. M. Bell. J. Phys. C *15*:1077 (1982).

35. P. Katbamna, L. J. Dunne, W. Ford, D. A. Lavis, and B. W. Southern. Phys. Stat. Sol. (b) *178*:335 (1993).
36. K. A. Dill and D. Stigter. Biochemistry *27*:3446 (1988).
37. D. Stigter and K. A. Dill. Langmuir *4*:200 (1988).
38. R. S. Cantor and K. A. Dill. Langmuir *2*:331 (1986).
39. E. Ruckenstein and B. Li. Langmuir *12*:2308 (1996).
40. S. Mafé, J. A. Manzanares, K. Kontturi. J. Electroanal. Chem. *457*:155 (1998).
41. D. Grandell and L. Murtomäki. Langmuir *14*:556 (1998).
42. J. Lipkowski, in *Modern Aspects of Electrochemistry*, vol. 23 (B. E. Conway, J. O'M. Bockris, and R. E. White, eds.) Plenum Press, New York, 1992, pp. 1–99.
43. C. J. Slevin, R. Ryley, D. J. Walton, and P. R. Unwin. Langmuir *14*:5331 (1998).
44. H. H. J. Girault and D. J. Schiffrin. J. Electroanal. Chem. *179*:277 (1984).
45. D. Grandell, L. Murtomäki, and G. Sundholm. J. Electroanal. Chem. *469*:72 (1999).
46. P. Liljeroth, A. Mälkiä, A. K. Kontturi, and K. Kontturi, in *Euroconference on Moder Trends in Electrochemistry of Molecular Interfaces*, Kirkkonummi, Finland, 1999, P-25.
47. D. Georganopoulou, J. Zhang, D. E. Williams, P. Unwin, and K. Kontturi, in *Euroconference on Modern Trends in Electrochemistry of Molecular Interfaces*, Kirkkonummi, Finland, 1999, P-17.
48. M. Tsionsky, A. J. Bard, and M. V. Mirkin. J. Am. Chem. Soc. *119*:10785 (1997).
49. M.-H. Delville, M. Tsionsky, and A. J. Bard. Langmuir *14*:2774 (1998).
50. L. Murtomäki, K. Kontturi, and D. J. Schiffrin. J. Electroanal. Chem. *474*:89 (1999).
51. I. Benjamin. Annu. Rev. Phys. Chem. *48*:407 (1997).
52. H. H. J. Girault and D. J. Schiffrin, in, *Electroanalytical Chemistry*, vol. 15 (A. J. Bard, ed.), Marcel Dekker, New York, 1989, pp. 1–141.
53. Z. Samec. J. Electroanal. Chem. *99*:197 (1979).
54. T. Kakiuchi, J. Noguchi, and M. Senda. J. Electroanal. Chem. *336*:137 (1992).
55. K. Kontturi, J. A. Manzanares, and L. Murtomäki. Electrochim. Acta *40*:2979 (1995).
56. J. D. Reid, O. R. Melro, and R. P. Buck. J. Electroanal. Chem. *147*:71 (1983).
57. B. d'Epenoux, P. Seta, G. Amblard, and C. Gavach. J. Electroanal. Chem. *99*:77 (1979).
58. A. Vincze, G. Horvai, and F. A. M. Leermakers. J. Phys. Chem. *100*:8946 (1996).
59. J. Strutwolf, J. A. Manzanares, and D. E. Williams. Electrochem. Commun. *1*:139 (1999).
60. A. N. Frumkin. Dokl. Akad. Nauk. SSSR *85*:373 (1952).
61. M. M. Standish and B. A. Pethica. Trans. Faraday Soc. *64*:1113 (1968).
62. R. G. Ashcroft, H. G. L. Coster, and J. R. Smith. Biochim. Biophys. Acta *643*:191 (1981).
63. T. Okada and J. M. Patil. Langmuir *14*:6241 (1998).
64. J. Seeling, P. M. Macdonald, and P. G. Scherer. Biochemistry *26*:7535 (1987).
65. F. H. Florenzano, and L. G. Dias. Langmuir *13*:5756 (1997).
66. M. da Silva Baptista, I. Cuccovia, H. Chaimovich, M. J. Politi, and W. F. Reed. J. Phys. Chem. *96*:6442 (1992).
67. A. Raudino and D. Mauzerall. Biophys. J. *50*:441 (1986).
68. C. Gavach, P. Seta, and B. d'Epenoux. J. Electroanal. Chem. *83*:225 (1977).
69. Z. Samec, T. Kakiuchi, and M. Senda. Electrochim. Acta *40*:2971 (1995).